Open access • Journal Article • DOI:10.1039/C2JM35148J

Exploiting high quality PEDOT:PSS–SWNT composite formulations for wet-spinning multifunctional fibers — Source link

Rouhollah Jalili, Joselito M. Razal, Gordon G. Wallace

Institutions: University of Wollongong

Published on: 20 Nov 2012 - Journal of Materials Chemistry (The Royal Society of Chemistry)

Topics: PEDOT:PSS, Carbon nanotube, Nanotube, Composite number and Fiber

1-1-2012

Exploiting high quality PEDOT:PSS-SWNT composite formulations for wet-spinning multifunctional fibers

Rouhollah Jalili
University of Wollongong, rjalili@uow.edu.au

Joselito M. Razal
University of Wollongong, jrazal@uow.edu.au

Gordon G. Wallace
University of Wollongong, gwallace@uow.edu.au

Exploiting high quality PEDOT:PSS-SWNT composite formulations for wet-spinning multifunctional fibers

Abstract

In order to exploit the inherent properties of carbon nanotubes (CNT) in any polymer composite, systematic control of carbon nanotube loading and protocols that mitigate against CNT bundling are required. If such composites are to be rendered in fiber form *via* wet-spinning, then CNT bundling during the coagulation process must also be avoided. Here we have achieved this by utilizing highly exfoliated single walled carbon nanotubes (SWNT) and poly(3,4-ethylenedioxythiophene):poly(styrenesulfonicacid) (PEDOT:PSS) to obtain wet-spinnable composite formulations at various nanotube volume fractions (V_f). The addition of only 0.02 V_f of aggregate-free and individually dispersed SWNT resulted in a significant enhancement of modulus, tensile strength, electrical conductivity and two cell electrode specific capacitance of PEDOT:PSS–SWNT composite fibers to 5.2 GPa, 200 MPa, 450 S cm^{-1} and 59 F g^{-1} by the rate of dY/dV_f = 89 GPa, $d\sigma/dV_f$ = 3.2 GPa, dS/dV_f = 13300 S cm^{-1} and 6 folds, respectively.

Keywords

composite, formulations, wet, exploiting, spinning, high, multifunctional, quality, pedot, pss, swnt, fibers

Disciplines

Engineering | Physical Sciences and Mathematics

Publication Details

Jalili, R., Razal, J. M. & Wallace, G. G. (2012). Exploiting high quality PEDOT:PSS-SWNT composite formulations for wet-spinning multifunctional fibers. Journal of Materials Chemistry, 22 (48), 25174-25182.

Journal of Materials Chemistry

Cite this: J. Mater. Chem., 2012, 22, 25174

www.rsc.org/materials

PAPER

Exploiting high quality PEDOT:PSS–SWNT composite formulations for wet-spinning multifunctional fibers†

Rouhollah Jalili, Joselito M. Razal* and Gordon G. Wallace*

Received 2nd August 2012, Accepted 3rd October 2012
DOI: 10.1039/c2jm35148j

In order to exploit the inherent properties of carbon nanotubes (CNT) in any polymer composite, systematic control of carbon nanotube loading and protocols that mitigate against CNT bundling are required. If such composites are to be rendered in fiber form *via* wet-spinning, then CNT bundling during the coagulation process must also be avoided. Here we have achieved this by utilizing highly exfoliated single walled carbon nanotubes (SWNT) and poly(3,4-ethylenedioxythiophene): poly(styrenesulfonicacid) (PEDOT:PSS) to obtain wet-spinnable composite formulations at various nanotube volume fractions (V_f). The addition of only 0.02 V_f of aggregate-free and individually dispersed SWNT resulted in a significant enhancement of modulus, tensile strength, electrical conductivity and two cell electrode specific capacitance of PEDOT:PSS–SWNT composite fibers to 5.2 GPa, 200 MPa, 450 S cm^{-1} and 59 F g^{-1} by the rate of $dY/dV_f = 89$ GPa, $d\sigma/dV_f = 3.2$ GPa, $dS/dV_f = 13\,300$ S cm^{-1} and 6 folds, respectively.

Introduction

Single wall carbon nanotubes (SWNT) have been used extensively in polymer composites with a view to improving mechanical and electrical properties while also providing thermal conductivity.[1–12] The addition of carbon nanotubes to wet-spun fibers provides materials in a practically useful form wherein enhancements in the above properties can be utilized.[8,13,14] One of the most successful methods used to prepare SWNT-based composite fibers *via* wet-spinning is to inject a surfactant stabilised SWNT dispersion into a bath that contains a polymer coagulant.[15–21] In this regard, a compromise in electrical conductivity, particularly for SWNT-based composite fibers that display excellent mechanical reinforcement, is observed. As an example, supertough PVA–SWNT fibers (prepared *via* the coagulation method), exhibit modulus, strength and toughness values as high as 80 GPa, 1.8 GPa and 570 J g^{-1}, respectively;[17] however, the electrical conductivity is low (~2.5 S cm^{-1}) a direct result of the adverse effect of PVA (an insulator) on the overall electrical conductivity.[17,19] Although the removal of PVA *via* thermal annealing can enhance the electrical conductivity, the mechanical properties are severely compromised.[18,19] However, it has been shown that when the polymer host is inherently conducting such as polyaniline and polypyrrole, the addition of SWNT during the fiber spinning process provides significant benefits including, but not limited to, high electrical conductivity in contrast with an insulator polymer host such as PVA.[22–25]

In a mechanically reinforced system, enhancement is generally achieved at low CNT loadings (typically 1 to 10% of SWNT).[16,26] To achieve considerable electrical conductivity, exceeding the percolation threshold, higher loadings (typically 10 to 80%) are required.[10,27] However, SWNT dispersions with highly exfoliated tubes (*i.e.* those with SWNT bundles <3 nm) are usually obtained and maintained at low concentrations (*i.e.* 0.1 mg ml^{-1}).[28] There is a need, therefore, to obtain both enhanced mechanical and electrical properties at low SWNT volume fractions.

Substituting inherently conducting polymers (ICPs) for PVA should be a step towards this goal. Reinforcement of ICPs with SWNT is also valuable in terms of electrical properties, as the conductivity of ICPs is limited in the reduced state. The SWNT (or multi walled nanotubes) can provide an effective conduit for charge delivery.[23,29,30] This ability is beneficial in applications that require electrochemical switching of the ICPs such as with high-strength artificial muscles.[22]

Poly(3,4-ethylenedioxythiophene):poly(styrenesulfonicacid) (PEDOT:PSS) can be made highly conductive, is environmentally stable and commercially available.[31] Here we investigate the effects of spinning formulations and processing parameters on the formation and subsequent properties of PEDOT:PSS–SWNT composite fibers. The method used to obtain the SWNT, the protocol used for addition of SWNT to the PEDOT:PSS and the loading level employed have been directly correlated to the quality and ease of spinnability of the formulations and to the mechanical and electrical properties of the resultant fibers.

Intelligent Polymer Research Institute, ARC Centre of Excellence for Electromaterials Science, AIIM Facility, Innovation Campus, University of Wollongong, Wollongong, NSW, 2522, Australia. E-mail: jrazal@uow.edu.au; gwallace@uow.edu.au; Fax: +61 2 4221 3114; Tel: +61 2 4221 3127

† Electronic supplementary information (ESI) available: Describes method used to wet-spin composite fibers with various loadings. Results and discussion on the electrical and mechanical properties of fibers with V_f >0.02. Tables S1 and S2 and Fig. S1–S4. See DOI: 10.1039/c2jm35148j

Experimental

Materials

The materials used in this work were all sourced commercially and used as received. Sodium dodecyl sulphate (SDS) is from BDH chemical, PEDOT:PSS chips are from Agfa under the trade name Orgacon dry (Lot. #A62 0000AC), purified HiPco SWNT are from Carbon Nanotechnologies Inc (Lot. # PO341).

Preparation of spinning solutions

SDS–SWNT stock dispersions were prepared (in 5 : 1 and 3 : 1 SDS : SWNT mass ratio) by adding the required SWNT amount in 5 mg ml^{-1} or 9 mg ml^{-1} SDS stock solution dissolved in Milli Q water to make 1 mg ml^{-1} and 3 mg ml^{-1} SWNT concentrations, respectively. These SDS–SWNT stock dispersions were subjected to 15 min of high-power tip sonication (SONICS Vibra Cell 500 W, 30% amplitude) followed by a 1 h low-power bath sonication (Branson B5500R-DTH) and then subjected to another 15 min high-power tip sonication before being allowed to rest overnight. Centrifugation (Eppendorf 5702) was carried out at 4400 rpm (3000*g*) for 90 min and the supernatant carefully decanted and saved. The post-centrifuge SWNT concentrations, determined from absorbance measurements at 660 nm,[28] were 0.5 mg ml^{-1} and 2.2 mg ml^{-1} for SDS–SWNT stock dispersions from the initial concentrations of 1 mg ml^{-1} and 3 mg ml^{-1}, respectively. All PEDOT:PSS–SWNT composite dispersions were subsequently prepared by adding the required amount of PEDOT:PSS chips to the SWNT stock solutions. The dispersions were stirred overnight followed by a 1 h low-power bath sonication (Table S1†).

Fiber spinning

The composite fibers were fabricated at room temperature using a wet-spinning technique as described previously.[32,33] Typically, about 5 ml of the spinning formulation in a syringe was extruded through a 20 gauge blunt needle (as a spinneret) into a coagulation bath (isopropanol) controlled by a syringe pump at flow rates between 0.8 and 2 mg h^{-1}. Fibers collected at the bottom of the coagulation bath were wound continuously onto a winding spool at a constant speed of 4 m min^{-1}. Post-treatment was carried out by wetting the as-spun fibers with ethylene glycol (EG) for 5 min and then oven drying at 150 °C for 30 min.

Characterization

The mechanical properties of the fibers were measured using a Shimadzu tensile tester (EZ-S) at a strain rate of 0.5% min^{-1}. Samples were mounted on aperture cards (1 cm length window) with commercial superglue and allowed to air dry. Youngs modulus (Y), tensile strength (σ), breaking strain (ε), and breaking energy (toughness) were calculated and the mean and standard deviation reported from 10 samples. A linear four-point probe conductivity cell with uniform 2.3 mm probe spacing was employed to measure the conductivity of the fibers (under laboratory humidity and temperature conditions) using a galvanostat current source (Princeton Applied Research Model 363) and a digital multimeter (HP Agilent 34401A). Electrochemical behavior of the PEDOT:PSS–SWNT composite fibers in deoxygenated organic electrolyte (0.1 M TBAP in acetonitrile) was investigated *via* CV using a potentiostat/galvanostat (Princeton Applied Research Model 363). A three-electrode cell constitutes a composite fiber working electrode, a $Ag/AgNO_3$ reference electrode and a platinum mesh auxiliary electrode. A symmetrical two electrode configuration constitutes composite fibers as cathode and anode. SEM microscopy images of fiber surfaces and tensile-fractured cross-sections were obtained using a field emission SEM (JEOL JSM-7500FA). Polarized Raman spectra were recorded on a Jobin Yvon Horiba HR800 Raman microscope using a 632 nm laser line and a 300-line grating to achieve a resolution of ± 1.25 cm^{-1}. Samples were fixed on a substrate and a set of reference spectra was recorded and then the polarizer is rotated 30° to record the next set of spectra. This rotation is repeated twice until the laser was polarized by 90°. In order to evaluate G′ band shift as a function of strain on the fibre, both ends of one fibre were glued on the tip of a caliper, then the caliper was secured on the Raman stage. The spectrum was recorded before and after applying strain via the caliper (up to 0.5%). Zetasizer (Nano-ZS, from Malvern Instruments Ltd) was used to measure the zeta potential of the spinning formulations.

Results and discussions

Building upon previously reported methods for continuous wet-spinning of highly conducting PEDOT:PSS fibers,[33,34] we demonstrate here that the addition of carbon nanotubes results in significant improvements in mechanical and electrical properties as well as electrochemical performance.

The spinning feed formulation and wet-spinning parameters

The spinning feed formulations were prepared by dissolving PEDOT:PSS pellets in pre-prepared aqueous stock dispersions of SDS–SWNT. Abrupt addition of PEDOT:PSS pellets into the SDS–SWNT dispersion resulted in the gelation of PEDOT:PSS–SWNT formulations and became unspinnable. Although the viscosity of this dispersion could be reduced by low power sonication, micron-sized aggregates still remained and further prevented effective fiber spinning. To avoid this problem, PEDOT:PSS pellets were dissolved gradually (stirred overnight at 500 rpm) in the SDS–SWNT dispersion followed by one hour bath sonication to remove air bubbles prior to spinning. Using a non-centrifuged SDS–SWNT stock dispersion containing 1 mg ml^{-1} SWNT and 5 mg ml^{-1} SDS, the maximum PEDOT:PSS concentration that can be achieved without gelation and aggregation was 12.5 mg ml^{-1}. This spinning feed formulation translates to a maximum achievable SWNT volume fraction in the fiber of 0.04 V_f. This SWNT V_f is based on the assumption that none of the spinning components was soluble in the coagulation bath *i.e.* no components were lost during the wet-spinning process. The composition of the spinning formulation was varied by the addition of different amounts of PEDOT:PSS pellets into the SDS–SWNT aqueous dispersion (Table S1†). It was observed that the resultant spinning feed formulations did not form any aggregates and was stable over a period of 7 days. The measured zeta potential of SDS–SWNT, PEDOT:PSS and PEDOT:

PSS–SWNT was −64.3 mV ± 12, −76.5 mV ± 6 and −70 mV ± 7, respectively. Such high zeta potentials have been shown to aid the stability of colloidal suspensions.[35] Note that PEDOT:PSS contains excess PSS that acts to maintain the PEDOT segments well-dispersed in water. Usually the PSS content is 2.5 times higher than PEDOT. The presence of excess PSS, which has also been reported to be a good dispersant for carbon nanotubes[36] is believed to facilitate the stability of the final PEDOT:PSS–SWNT composite formulation.

The preparation of the above wet-spinnable SWNT-composite formulations (*i.e.* the direct addition of PEDOT:PSS into SWNT dispersions) is straightforward and allows the control over the spinning feed composition and quality (*i.e.* homogeneity of SWNTs in the polymer can be evaluated) prior to the actual wet-spinning process. Several biopolymer-based spinning formulations have been prepared in this manner but those reports did not investigate the effect of nanotube loading in the fiber properties.[13,14,37–40] The most commonly employed strategy is wet-spinning a surfactant-based SWNT dispersion into a polymer coagulant.[41] The polymer–SWNT composition of the resultant composite fiber using this latter method could not be precisely controlled and typically results in a CNT loading of ~60 wt% (or ~0.5 V_f).[17] This strategy has been applied to a limited number of polymers such as PVA and epoxy.[17,42] On the other hand, melt-processing of homogeneous SWNT–polymer also requires a relatively complex procedure. Haggenmueller *et al.* also dispersed SWNT and poly(methyl methacrylate) (PMMA) in dimethylformamide (DMF), then blended the mixtures and finally cast the final product.[43] The resultant films were chopped, melted and cast again. This procedure was then repeated twenty five times to improve the dispersion of SWNT before spinning composite fibers.

In spinning the PEDOT:PSS–SWNT formulations, we used the previously described wet-spinning set-up for pure PEDOT:PSS fibers.[33] In this set-up, the PEDOT:PSS–SWNT spinning feed was injected through a 20 gauge needle from the top of a vertical glass column to a second collection bath (both containing the coagulation bath). In this work, several organic solvents were initially investigated as coagulation bath but it was found that the use of isopropanol (IPA) resulted in continuous fibers with uniform circular cross-section along the fiber length (Fig. 3A). It was also found that a spinning feed rate of 2 ml h^{-1} and a take-up speed (for fiber collection) of around 1 to 2 m h^{-1} resulted in continuous fiber production. In contrast to the previous report where the lowest spinnable PEDOT:PSS concentration was 20 mg ml^{-1},[33] we found that the composite formulation containing 12.5 mg ml^{-1} PEDOT:PSS was spinnable. This positive contribution of SWNT on the spinnability was due to the further cohesion which was obtained by adding SWNT to the spinning formulation.

The stress–strain curves obtained for as-spun PEDOT:PSS–SWNT composite fibers indicated a clear improvement in mechanical properties in comparison to pure PEDOT:PSS fibers (Fig. 1A). Both strength and modulus increased by 54% and 157%, respectively; the breaking strain, however, was reduced by 50%. The reduction in breaking strain could be attributed to the presence of non-exfoliated SWNTs (*i.e.* large SWNT bundles).

We employed a mild centrifugation process to separate and remove aggregates and large SWNT bundles from the stock SDS–SWNT dispersion prior to the addition of PEDOT:PSS

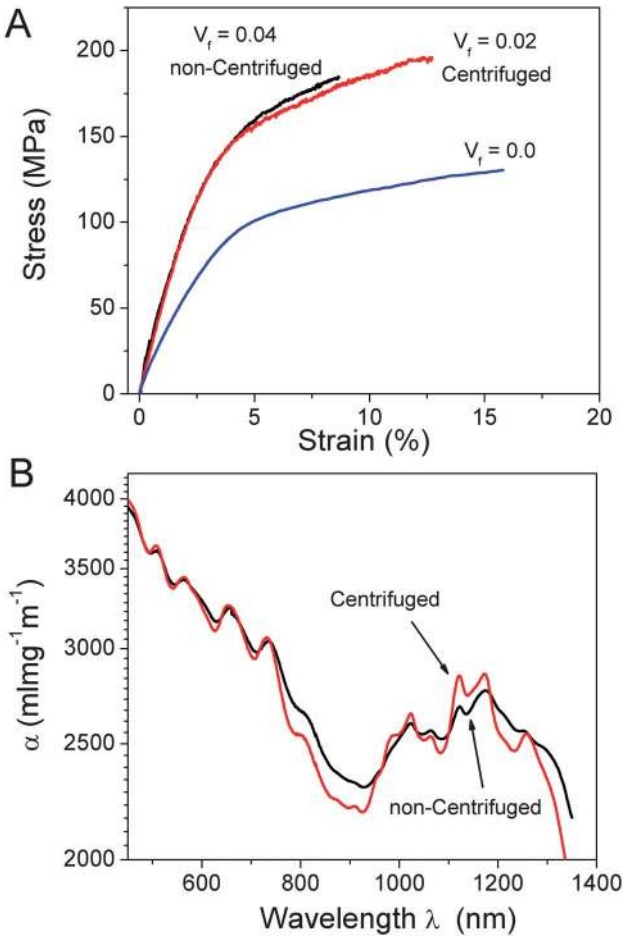

Fig. 1 (A) Representative stress–strain curves of fibers prepared from as-prepared PEDOT:PSS fiber, fiber with $V_f = 0.04$ of non-centrifuged SDS–SWNT dispersion, and fiber with $V_f = 0.02$ of centrifuged SDS–SWNT dispersion. (B) UV-VIS-NIR spectra of SDS–SWNT-dispersion before and after centrifugation.

pellets. We found that by using centrifugation parameters of 3300 rpm for 90 min, a stable SDS–SWNT supernatant with a SWNT concentration of 0.5 mg ml^{-1} could be achieved, in agreement with previous reports.[35] Literature reports show that by using a mild centrifugation process, the bundle size of SWNTs that remained in the dispersion decrease with centrifugation rate and time.[35]

The well-resolved inter-band transitions in the UV-VIS spectra of the centrifuged SDS–SWNT dispersions (Fig. 1B) indeed indicated the presence of individual and/or very small SWNT bundles.[35] This result is advantageous for composites because when the high quality SWNT dispersion was employed for fiber spinning, the higher effective reinforcing surface area of the individual/small SWNT bundles could lead to close to ideal improvements in mechanical properties.[8] Furthermore, the removal of SWNT aggregates could alleviate stress–concentration points and defect sites along the fiber length and higher breaking strains and toughness (breaking energy) could be attained.[16] The properties obtained for the composite fibers after centrifugation of the SWNT dispersion confirmed this with an enhancement of the toughness by 20% (from 15.9 to 19 J g^{-1}) and higher breaking strain (12% compared to 9% for non-centrifuged

sample) recorded. It is noteworthy that these improvements in properties are observed despite the fact that ~50% of the initial SWNT concentration decreased after centrifugation (resulting in a SWNT loading of 0.02 V_f in the composite fiber, Table S1†). When fibers of equivalent SWNT loadings were compared, the modulus and strength were ~25% higher for the composite fiber that contained the SWNT from a centrifuged dispersion.

Another striking result is the demonstrated ability to prevent SWNT from aggregating in the composite fibers. The composite fibers fabricated from "cleaned-up" centrifuged SDS–SWNT stock dispersions exhibited an aggregate-free morphological structure A (Fig. 2A–C). Only individual/small SWNT bundles were observed on fibers prepared from the centrifuged SWNT dispersion. Some small SWNT bundles were present in fibers prepared using the non-centrifuged SDS–SWNT dispersion, however, large SWNT bundles and aggregates were more dominant (Fig. 2F). From here on, the fibers described in the succeeding sections were prepared from centrifuged SDS–SWNT stock dispersions.

Since our aim is to evaluate the reinforcement effect of SWNTs in the composite fibers, it is necessary to prepare composite fibers with various SWNT loading. In order to make composite fibers with SWNT loading with V_f >0.02, a second SDS–SWNT stock dispersion was prepared (see Experimental section). It is quite evident that distinct differences in the shape and microstructure of the PEDOT:PSS–SWNT composite fibers could be correlated with the concentration of the SDS–SWNT stock dispersion used and hence, the SWNT loading of the resultant fiber (Fig. 3). All fibers with SWNT V_f ≤0.02 (*i.e.* fibers prepared from a SDS–SWNT stock dispersion with 0.5 mg ml^{-1} SWNT) showed compact and circular fibers. Fibers with SWNT V_f >0.02 (*i.e.* the employed SDS–SWNT stock dispersion contained 2.2 mg ml^{-1} SWNT) resulted in fluffy, porous and irregularly shaped fibers. Close inspection of the fiber morphology revealed that composite fibers with SWNT loading of 0.02 < V_f ≤ 0.09 resulted in phase segregation as manifested by the SWNT-rich and SWNT-poor regions. The SEM images also revealed that the SWNT bundles in composite fibers with SWNT V_f >0.02 are larger than those observed in fibers containing SWNT V_f ≤0.02. This observation is in agreement with the previously reported SWNT bundle size dependence on SWNT concentration.[28] For the two SDS–SWNT stock concentrations employed in this work (*i.e.* SWNT concentrations of 0.5 and 2.2 mg ml^{-1}), the average SWNT bundle size was previously estimated to be ~7 and ~14 nm, respectively.[28] In addition, the SDS content was estimated to be ~2 times difference between the two SDS–SWNT stock dispersions (Table S1†), which could explain the highly porous microstructure of the composite fiber prepared with high SDS content.

Mechanical properties

A number of papers have shown that improving the alignment of SWNT can result in an overall improvement in mechanical properties and specifically the modulus of the composite fibers.[15,16,44–46] For fibers obtained here, alignment of the SWNT was observed. As can be seen from Fig. 4A–C, when fibers are broken under tensile test, large number of oriented nanotubes are protruding from the fracture surface. We also used polarized Raman spectroscopy to monitor the orientation of SWNT along the fibers axis (Fig. 4D). The intensity of the tangential mode G band (1592 cm^{-1}) in the polarized Raman spectra monotonically decreased with increasing the angle between the fiber axis and the polarization direction confirming the orientation of SWNT.[44,47] The comparison of mechanical properties of PEDOT:PSS–SWNT composite fibers as a function of SWNT loading is shown

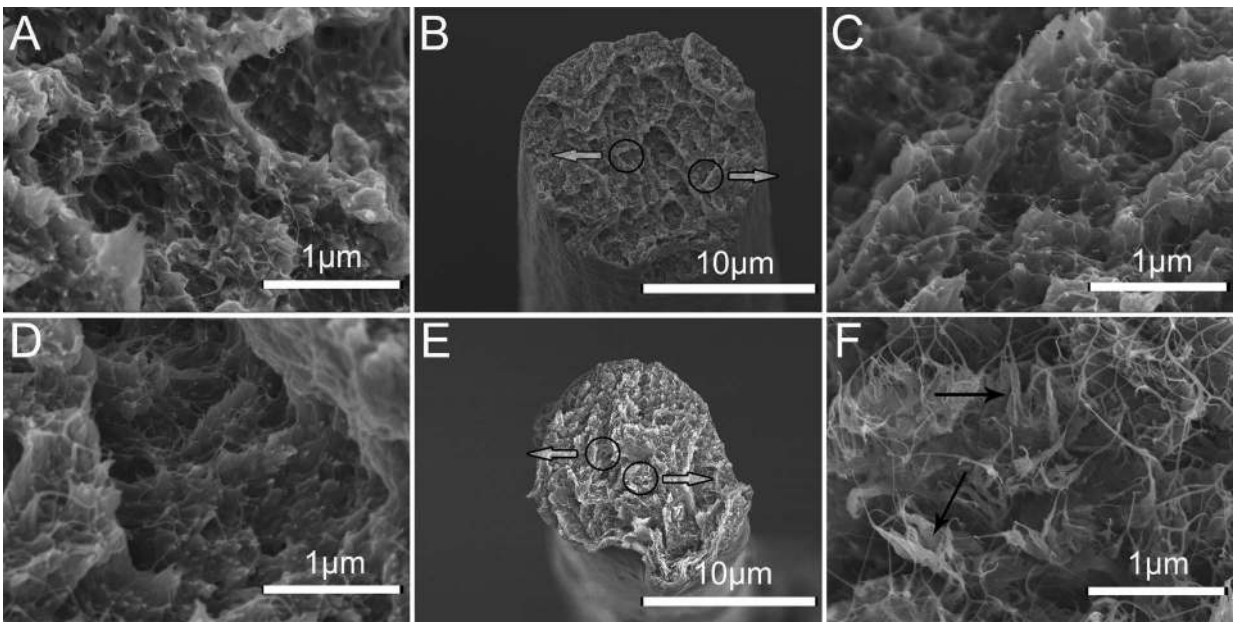

Fig. 2 SEM images of the cross-sections of PEDOT:PSS–SWNT composite fibers broken under tensile strain prepared from (A–C) centrifuged SDS–SWNT stock dispersion and (D–F) non centrifuged SDS–SWNT stock dispersions. Arrows are pointed from the magnified spots for each sample. As can be seen in (F) there are some nanotube aggregates in the non-centrifuged sample which are shown by arrows. However, in the centrifuged sample (A and C) nanotubes appear to be well dispersed in the polymer matrix.

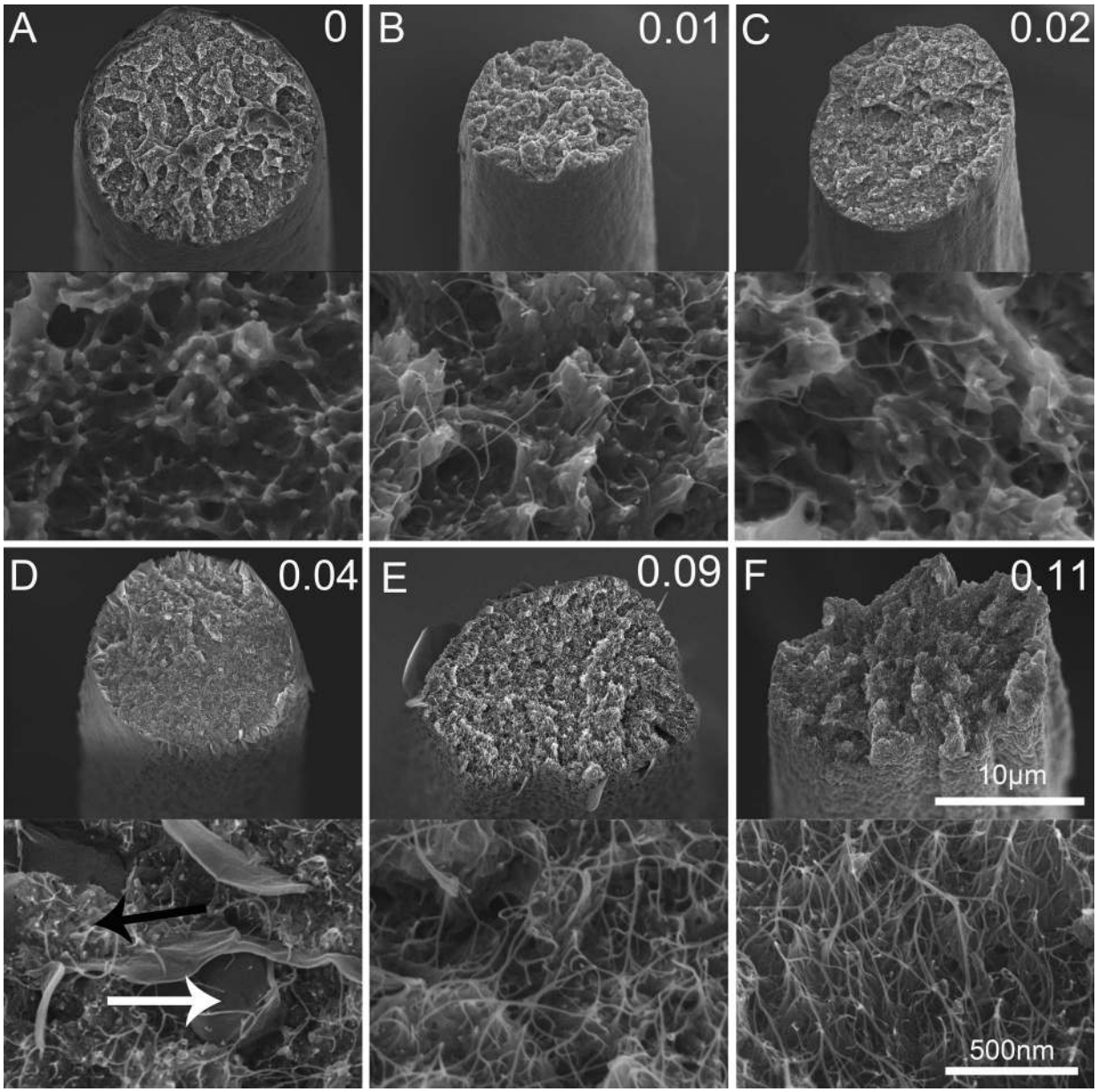

Fig. 3 Cross-section of tensile fractured PEDOT:PSS–SWNT composite fibers at low and high magnifications showing transformations of shape and microstructure of PEDOT:PSS composite fiber upon the addition of SWNT at various loadings. Volume fraction of SWNT indicated on each pair of images. White and black arrows at D shows PEDOT:PSS and SDS–SWNT rich region, respectively. Scale bars are similar for all images in each series.

in Fig. 5. Here the modulus of the composite fiber was doubled ($dY/dV_f = 89$ GPa) as a result of the alignment of the SWNT. The slope of the linear fit of modulus/strength at different V_f (Fig. 5) is an indication of the degree of reinforcement.[8,9,16] At $V_f = 0.02$, the tensile strength was found to be ~200 MPa and the degree of reinforcement ($d\sigma/dV_f$) was 3.2 GPa, which is higher than the values reported for PVA–SWNT based fibers[16] but lower than drawn and crystallized PVA–SWNT based fibers.[48] The observed increase in the tensile strength (Fig. 5B) was direct confirmation of maintaining the quality of dispersed SWNT into the bulk fibers even after composite production and spinning process.

In order to monitor the interfacial stress transfer between SWNT and polymer matrix, Raman spectroscopy was carried out. It has been shown that, as the composite fibre is strained, the position of G′ band tends to shift linearly with the deformation rate (strain) of the composite.[49,50] The position of G′ band (2614 cm^{-1}) of SWNT showed 2 cm^{-1} down-shift to lower wavenumber at 0.05% axial strain (Fig. S1†). This shift confirmed the contribution of SWNTs to load bearing due to a good interfacial interaction between SWNT and PEDOT:PSS matrix.

The strain-at-break did not decrease significantly by the addition of SWNT (Fig. 5C). This has been reported previously for PVA–SWNT based fibers and is opposite to the behaviour typically observed in classic composites.[15,44,47] Filling of a ductile polymer by rigid fillers usually improves the strength, but adversely affects ductility because rigid fillers (or large bundles of SWNT) act as stress concentration points where failure is

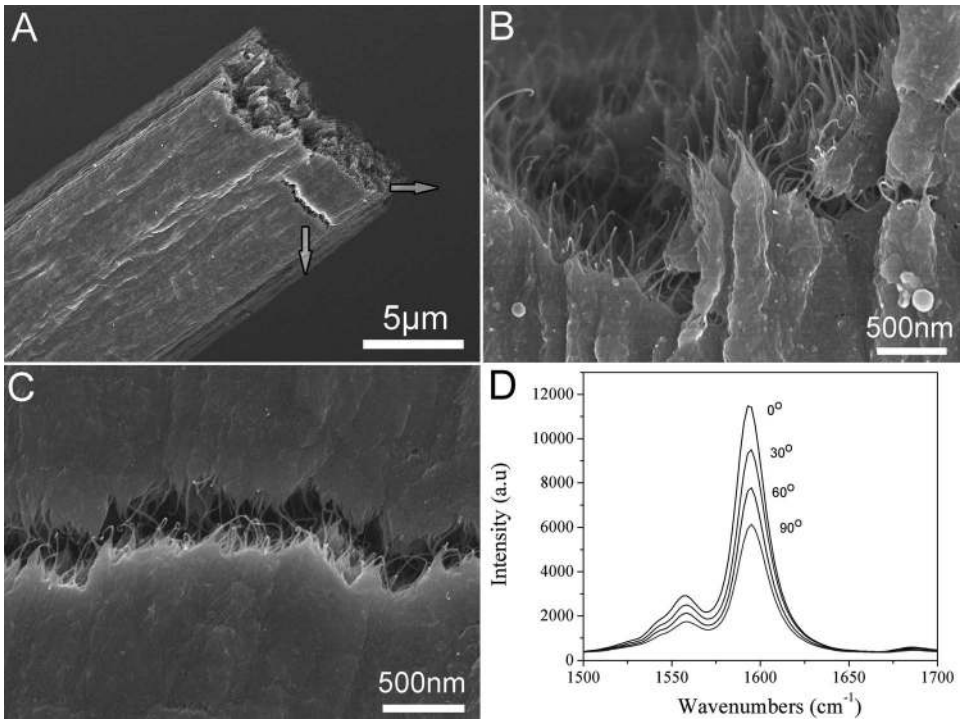

Fig. 4 (A–C) SEM images of a broken fiber. Arrows are pointed from the magnified spots. (D) Polarized Raman spectra of PEDOT:PSS–SWNT composite fibers. Single and straight fiber selected for the orientation-dependent measurements at different angles α_i between the polarization (electric field) of the incident laser light and the fiber axis. All measurements show maximum intensity when the polarization of the incident radiation is parallel to the fiber axis ($\alpha_i = 0°$), while near 90° the signal decreased to lowest intensity. Numbers shown refer to the polarization angle of the incident laser beam. The spectra are normalized to the D band (1359 cm^{-1}).

initiated. In contrast, individually dispersed oriented flexible SWNT in the polymer matrix (as confirmed by the SEM images and Raman spectroscopy) serve as reinforcing fillers and provide strengthening effect without the loss of ductility. This result highlights the advantage of the fabrication technique in maintaining the SWNT dispersion quality and using the shear forces encountered to aid in SWNT orientation along the fiber axis.

Another measure of a good reinforced composite is toughness (the total energy required to break the fiber composite), which depends on both strength and breaking strain of the material. The toughness of composite fibers (Fig. 5D) followed the same trend as modulus and strength. The highest toughness was measured at 0.02 V_f (19 J g^{-1}) which was ~20% higher than the pure PEDOT:PSS fiber (15.9 J g^{-1}). Nevertheless, to the best of the authors' knowledge, this toughness is by far the best reported toughness for a highly conducting SWNT-based composite fiber (those with conductivity above 300 S cm^{-1}).[14] Other highly conducting SWNT-based composite fibers that fall in this category have toughness of ≤10 J g^{-1}.[14,19,22]

Electrical conductivity

Electrical conductivity was enhanced by increasing the volume fraction of SWNT (Fig. 6). A sharp increase in conductivity reaching up to 450 S cm^{-1}, with the conductivity enhancement rate of dS/dV_f = 13 300 S cm^{-1} was observed. This effective contribution of SWNT to the total conductivity was more than 4 orders of magnitude higher than PVA–SWNT-based composites ($dS/dV_f \sim 1$ S cm^{-1})[27] and much higher than other insulator–SWNT-based composite films (up to $dS/dV_f \sim 500$ S cm^{-1}),[10] which were calculated based on the loading of SWNT and conductivity enhancement reported in the literature.[10] In an effectively reinforced polymer–SWNT system, each SWNT is individually coated with a layer of polymer to afford an efficient load transfer between tubes and matrix.[9] In this case, the efficiency of charge transfer within the adjacent SWNT is strictly limited.[27] When such a resistive barrier is present, the charge transport is not efficient and happens only by fluctuation induced tunnelling.[51] On the other hand, much higher electron transport efficiency between the adjacent PEDOT:PSS-coated SWNT was obtained due to the conductivity of the PEDOT:PSS matrix itself.

It is noteworthy that most of the highly conducting SWNT-based composite fibers can achieve high conductivity when filled with at least 50 wt% SWNT (Table S2†), these loadings are far higher than V_f 0.02 (~3 wt%) presented in this study. The addition of much lower amount of SWNT while obtaining the high levels of conductivity makes wet-spinning of PEDOT:PSS–SWNT fibers an economical and viable choice. The outstanding electrical conductivity of these fibers places them among the most conducting SWNT-based composite fibers and[14,22,38,39,52] comparable with the most successful SWNT-reinforced composites reported to date.[7,13–16,38,53–59]

Electrochemical performance

The electrochemical behavior of the fibers was investigated using cyclic voltammetry. This study evaluates the additional benefits

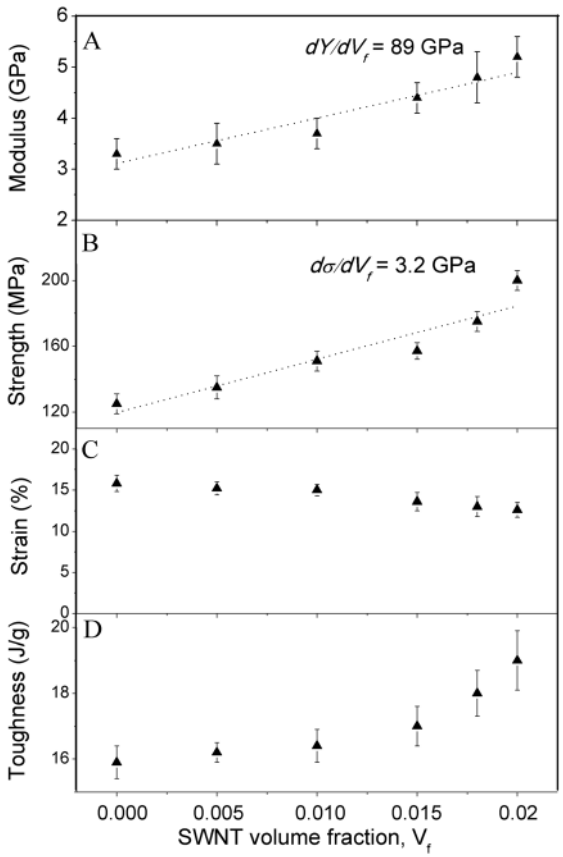

Fig. 5 Comparison of the mechanical properties of PEDOT:PSS–SWNT composite fibers as a function of SWNT loading. The lines in A and B are the linear fits to the data.

gained from using SWNT as mechanical and electrical reinforcing agents. Both three-electrode and two-electrode (symmetric) cells were used to evaluate electrochemical properties; the latter test configuration is valuable in estimating the capacitance of the fibers when used as electrode(s) in an electrochemical supercapacitor device. The highest SWNT loading of 0.02 V_f was selected to perform electrochemical tests as both best mechanical properties and electrical conductivity were observed in this loading. The cyclic voltammograms (CVs) of fibers characterized in a three-electrode configuration revealed Faradaic responses typical of a pure PEDOT:PSS material (Fig. 7A). The oxidation (−0.4 and +0.3 V *vs.* Ag/Ag^+) and reduction peaks (−0.2 and −0.4 V *vs.* Ag/Ag^+) are similar to those reported previously.[33,60] The more clearly defined redox peaks in the CV relate to the enhanced conductivity of PEODT:PSS fiber after the addition of SWNT. Also evident is the increased specific current response and a rectangular-shape CV of composite fibers indicative of the ease of ion transport through the bulk of the fiber during oxidation and reduction due to the introduction of carrier-transporting channels through the polymer by SWNT.[29]

In the two-electrode configuration (Fig. 6B), the capacitive behavior of fibers was represented by the near-rectangular shaped CVs at the scan rate of 50 mV s^{-1} confirming that the overall internal resistance is low, owing to the improved fiber conductivity *via* SWNT addition. Significant improvement in the specific capacitance after SWNT addition was observed (Table 1). In comparison to the specific capacitance (two-electrode cell) of pure PEDOT:PSS fiber (10 F g^{-1}), value of V_f 0.02 resulted to approximately six-fold (59 F g^{-1}) increase in the specific capacitance of composite fibers consistent with the electrical conductivity enhancement discussed before.

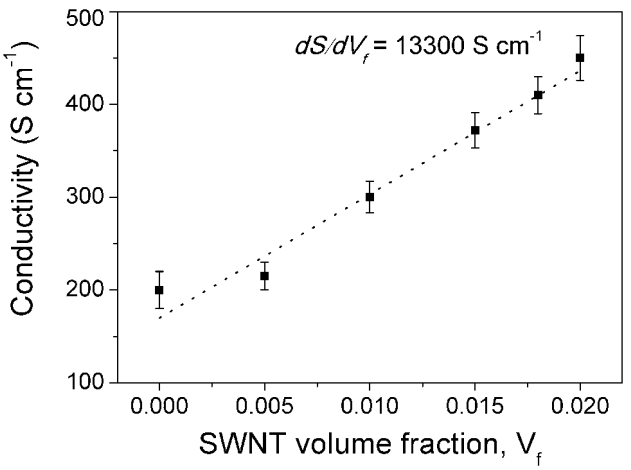

Fig. 6 Comparison of the electrical properties of PEDOT:PSS–SWNT composite fibers as a function of SWNT loading.

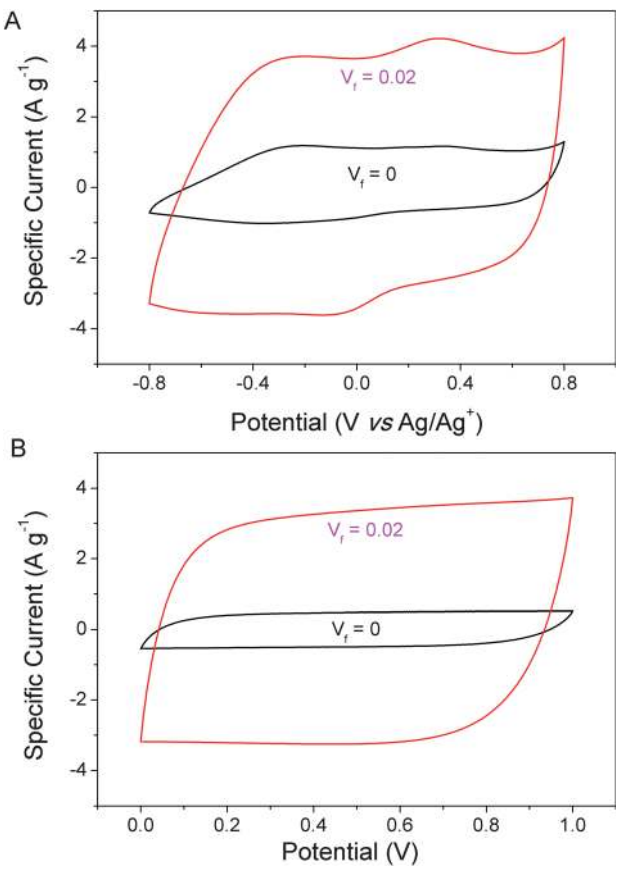

Fig. 7 CV of PEDOT:PSS–SWNT composite fibers as a function of SWNT loading in 0.1 M $TBABF_4$/acetonitrile taken at a scan rate of 50 mV s^{-1}. (A) Three-electrode cell system when potential measured *vs.* $Ag/AgNO_3$. (B) Two-electrode (symmetric) cell.

Table 1 Summary of electrochemical performance of PEDOT:PSS–SWNT composite fibers

Fiber type	SWNT loading [V_f]	Conductivity [S cm^{-1}]	dS/dV_f [S cm^{-1}]	Specific capacitance [F g^{-1}]		Capacitance retention[a] [%]
				3 Electrode	2 Electrode	
PEDOT:PSS	0	200 ± 20	NA	15	10	86.7
PEDOT:PSS–SWNT	0.02	450 ± 24	13 300	67	59	94.4

[a] After 500 cycles.

Comparing the specific capacitance of composite fibers with PEDOT:PSS–CNT paper,[61–63] CNT paper[64] and CNT fibers[52] reported in the literature, reveals a better or similar performance achieved for the composite fibers with a much lower SWNT loading. The improved performance may result from the coagulation process when a displacement between water and isopropanol occurred in the coagulation bath. This phenomenon transforms the spinning solution into a coagulated fiber with several micro voids and channels inside the PEDOT:PSS–SWNT fibers (Fig. 3). Therefore, ions can diffuse quickly through the micro- and nano-pores and can penetrate into the fibers easily.

The use of SWNT additive provided further benefit by improving the stability of the fiber electrodes during repeated cycling. The stability of the enhanced ionic and electronic transport of the composite fibers depicts a strong interaction between the aromatic SWNT and the π-conjugated PEDOT:PSS polymer chains.

Conclusions

We believe the current work is the first that has comprehensively measured both mechanical and electrical properties of wet-spun fibers as a function of SWNT volume fraction allowing accurate measurement of dY/dV_f, dσ/dV_f and dS/dV_f in the linear region as a result of the compatibility between the polymer matrix and composite formulation and processing method. The use centrifuged SWNT dispersions, has prevented the formation of SWNT aggregates during fiber spinning and therefore, reduced stress–concentration points and defect sites within the fiber resulting in enhanced toughness and rate of strength, modulus and conductivity reinforcements. Moreover, the high conductivity of PEDOT:PSS matrix facilitated electron transport efficiency between the adjacent SWNT leading to a significantly higher conductivity enhancement and electrochemical capacitance compared with literature reports. PEDOT:PSS–SWNT composite fibers were also used to fabricate electrochemical storage devices. These exciting properties present a range of opportunities for the development of macroscopic architectures in the areas of energy storage and conversion,[14,65] bionics[32,43] and biomedical devices.[42] It is also anticipated that the methods and results presented here is sufficiently general to provide useful strategies in solving the fundamental challenges commonly encountered in processing SWNT-based composites. We anticipate that these findings can be used as a guideline for rational design of multifunctional fibers for technological applications.

Acknowledgements

The authors thank the Australian Research Council (ARC) for financial support and the ANFF Materials Node for their provision of research facilities. The authors acknowledge use of the facilities and the assistance of Mr Tony Romeo at the UOW Electron Microscopy Centre. The authors thank Mrs Dorna Esrafilzadeh for her assistance in fiber spinning and Mr Seyed Hamed Aboutalebi for discussions. This work was supported by ARC APD Fellowship DP098753 (J.M. Razal).

Notes and references

1 Y. Yan, J. Cui, S. Zhao, J. Zhang, J. Liu and J. Cheng, *J. Mater. Chem.*, 2012, **22**, 1928–1936.
2 I. Firkowska, A. Boden, A.-M. Vogt and S. Reich, *J. Mater. Chem.*, 2011, **21**, 17541–17546.
3 R. E. Anderson, J. Guan, M. Ricard, G. Dubey, J. Su, G. Lopinski, G. Dorris, O. Bourne and B. Simard, *J. Mater. Chem.*, 2010, **20**, 2400–2407.
4 M. in het Panhuis, *J. Mater. Chem.*, 2006, **16**, 3598–3605.
5 H. Qian, E. S. Greenhalgh, M. S. P. Shaffer and A. Bismarck, *J. Mater. Chem.*, 2010, **20**, 4751–4762.
6 P. M. Ajayan, L. S. Schadler, C. Giannaris and A. Rubio, *Adv. Mater.*, 2000, **12**, 750–753.
7 T. B. Michele and K. G. k. Yurii, *Adv. Mater.*, 2009, **22**, 1672–1688.
8 J. N. Coleman, U. Khan and Y. K. Gun'ko, *Adv. Mater.*, 2006, **18**, 689–706.
9 J. N. Coleman, U. Khan, W. J. Blau and Y. K. Gun'ko, *Carbon*, 2006, **44**, 1624–1652.
10 W. Bauhofer and J. Z. Kovacs, *Compos. Sci. Technol.*, 2009, **69**, 1486–1498.
11 S. De, P. E. Lyons, S. Sorel, E. M. Doherty, P. J. King, W. J. Blau, P. N. Nirmalraj, J. J. Boland, V. Scardaci, J. Joimel and J. N. Coleman, *ACS Nano*, 2009, **3**, 714–720.
12 A. B. Dalton, S. Collins, J. Razal, E. Munoz, V. H. Ebron, B. G. Kim, J. N. Coleman, J. P. Ferraris and R. H. Baughman, *J. Mater. Chem.*, 2004, **14**, 1–3.
13 A. J. Granero, J. M. Razal, G. G. Wallace and M. i. h. Panhuis, *Adv. Funct. Mater.*, 2008, **18**, 3759–3764.
14 J. M. Razal, K. J. Gilmore and G. G. Wallace, *Adv. Funct. Mater.*, 2008, **18**, 61–66.
15 K. Young, F. M. Blighe, J. J. Vilatela, A. H. Windle, I. A. Kinloch, L. Deng, R. J. Young and J. N. Coleman, *ACS Nano*, 2010, **4**, 6989–6997.
16 F. M. Blighe, K. Young, J. J. Vilatela, A. H. Windle, I. A. Kinloch, L. Deng, R. J. Young and J. N. Coleman, *Adv. Funct. Mater.*, 2011, **21**, 364–371.
17 A. B. Dalton, S. Collins, E. Munoz, J. M. Razal, V. H. Ebron, J. P. Ferraris, J. N. Coleman, B. G. Kim and R. H. Baughman, *Nature*, 2003, **423**, 703.
18 E. Muñoz, A. B. Dalton, S. Collins, M. Kozlov, J. Razal, J. N. Coleman, B. G. Kim, V. H. Ebron, M. Selvidge, J. P. Ferraris and R. H. Baughman, *Adv. Eng. Mater.*, 2004, **6**, 801–804.
19 E. Muñoz, D. S. Suh, S. Collins, M. Selvidge, A. B. Dalton, B. G. Kim, J. M. Razal, G. Ussery, A. G. Rinzler, M. T. Martínez and R. H. Baughman, *Adv. Mater.*, 2005, **17**, 1064–1067.

20 J. M. Razal, J. N. Coleman, E. Muñoz, B. Lund, Y. Gogotsi, H. Ye, S. Collins, A. B. Dalton and R. H. Baughman, *Adv. Funct. Mater.*, 2007, **17**, 2918–2924.
21 C. Mercader, V. Denis-Lutard, S. Jestin, M. Maugey, A. Derré, C. Zakri and P. Poulin, *J. Appl. Polym. Sci.*, 2012, **125**, E191–E196.
22 G. M. Spinks, V. Mottaghitalab, M. Bahrami-Samani, P. G. Whitten and G. G. Wallace, *Adv. Mater.*, 2006, **18**, 637–640.
23 V. Mottaghitalab, G. M. Spinks and G. G. Wallace, *Polymer*, 2006, **47**, 4996–5002.
24 V. Mottaghitalab, G. M. Spinks and G. G. Wallace, *Synth. Met.*, 2005, **152**, 77–80.
25 J. Foroughi, G. M. Spinks and G. G. Wallace, *J. Mater. Chem.*, 2011, **21**, 6421–6426.
26 J. N. Coleman, M. Cadek, R. Blake, V. Nicolosi, K. P. Ryan, C. Belton, A. Fonseca, J. B. Nagy, Y. K. Gun'ko and W. J. Blau, *Adv. Funct. Mater.*, 2004, **14**, 791–798.
27 Y. R. Hernandez, A. Gryson, F. M. Blighe, M. Cadek, V. Nicolosi, W. J. Blau, Y. K. Gun'ko and J. N. Coleman, *Scr. Mater.*, 2008, **58**, 69–72.
28 S. D. Bergin, V. Nicolosi, H. Cathcart, M. Lotya, D. Rickard, Z. Sun, W. J. Blau and J. N. Coleman, *J. Phys. Chem. C*, 2008, **112**, 972–977.
29 S. Bhandari, M. Deepa, A. K. Srivastava, A. G. Joshi and R. Kant, *J. Phys. Chem. B*, 2009, **113**, 9416–9428.
30 C. Peng, J. Jin and G. Z. Chen, *Electrochim. Acta*, 2007, **53**, 525–537.
31 S. Kirchmeyer and K. Reuter, *J. Mater. Chem.*, 2005, **15**, 2077–2088.
32 J. M. Razal, M. Kita, A. F. Quigley, E. Kennedy, S. E. Moulton, R. M. I. Kapsa, G. M. Clark and G. G. Wallace, *Adv. Funct. Mater.*, 2009, **19**, 3381–3388.
33 R. Jalili, J. M. Razal, P. C. Innis and G. G. Wallace, *Adv. Funct. Mater.*, 2011, **21**, 3363–3370.
34 H. Okuzaki, Y. Harashina and H. Yan, *Eur. Polym. J.*, 2009, **45**, 256–261.
35 Z. Sun, V. Nicolosi, D. Rickard, S. D. Bergin, D. Aherne and J. N. Coleman, *J. Phys. Chem. C*, 2008, **112**, 10692–10699.
36 S. Razdan, P. K. Patra, S. Kar, L. Ci, R. Vajtai, A. K. Kukovecz, Z. N. Kónya, I. Kiricsi and P. M. Ajayan, *Chem. Mater.*, 2009, **21**, 3062–3071.
37 A. J. Granero, J. M. Razal, G. G. Wallace and M. in het Panhuis, *J. Mater. Chem.*, 2010, **20**, 7953–7956.
38 J. N. Barisci, M. Tahhan, G. G. Wallace, S. Badaire, T. Vaugien, M. Maugey and P. Poulin, *Adv. Funct. Mater.*, 2004, **14**, 133–138.
39 C. Lynam, S. E. Moulton and G. G. Wallace, *Adv. Mater.*, 2007, **19**, 1244–1248.
40 D. Y. Lewitus, J. Landers, J. R. Branch, K. L. Smith, G. Callegari, J. Kohn and A. V. Neimark, *Adv. Funct. Mater.*, 2011, **21**, 2624–2632.
41 B. Vigolo, A. Pénicaud, C. Coulon, C. Sauder, R. Pailler, C. Journet, P. Bernier and P. Poulin, *Science*, 2000, **290**, 1331–1334.
42 S. E. Moulton, M. J. Higgins, R. M. I. Kapsa and G. G. Wallace, *Adv. Funct. Mater.*, 2012, **22**, 2003–2014.
43 R. Haggenmueller, H. H. Gommans, A. G. Rinzler, J. E. Fischer and K. I. Winey, *Chem. Phys. Lett.*, 2000, **330**, 219–225.
44 Z. Wang, P. Ciselli and T. Peijs, *Nanotechnology*, 2007, **18**, 455709.
45 S. D. Bergin, V. Nicolosi, P. V. Streich, S. Giordani, Z. Sun, A. H. Windle, P. Ryan, N. P. P. Niraj, Z.-T. T. Wang, L. Carpenter, W. J. Blau, J. J. Boland, J. P. Hamilton and J. N. Coleman, *Adv. Mater.*, 2008, **20**, 1876–1881.
46 P. Miaudet, S. Badaire, M. Maugey, A. Derré, V. Pichot, P. Launois, P. Poulin and C. Zakri, *Nano Lett.*, 2005, **5**, 2212–2215.
47 J. R. Wood, Q. Zhao and H. D. Wagner, *Composites, Part A*, 2001, **32**, 391–399.
48 M. L. Minus, H. G. Chae and S. Kumar, *Macromol. Chem. Phys.*, 2009, **210**, 1799–1808.
49 C. A. Cooper, R. J. Young and M. Halsall, *Composites, Part A*, 2001, **32**, 401–411.
50 W. Ma, L. Liu, Z. Zhang, R. Yang, G. Liu, T. Zhang, X. An, X. Yi, Y. Ren, Z. Niu, J. Li, H. Dong, W. Zhou, P. M. Ajayan and S. Xie, *Nano Lett.*, 2009, **9**, 2855–2861.
51 B. E. Kilbride, J. N. Coleman, J. Fraysse, P. Fournet, M. Cadek, A. Drury, S. Hutzler, S. Roth and W. J. Blau, *J. Appl. Phys.*, 2002, **92**, 4024–4030.
52 M. E. Kozlov, R. C. Capps, W. M. Sampson, V. H. Ebron, J. P. Ferraris and R. H. Baughman, *Adv. Mater.*, 2005, **17**, 614–617.
53 S. Kumar, H. Doshi, M. Srinivasarao, J. O. Park and D. A. Schiraldi, *Polymer*, 2002, **43**, 1701–1703.
54 X. Zhang, T. Liu, T. V. Sreekumar, S. Kumar, X. Hu and K. Smith, *Polymer*, 2004, **45**, 8801–8807.
55 M. Naraghi, T. Filleter, A. Moravsky, M. Locascio, R. O. Loutfy and H. D. Espinosa, *ACS Nano*, 2010, **4**, 6463–6476.
56 R. Andrews, D. Jacques, A. M. Rao, T. Rantell, F. Derbyshire, Y. Chen, J. Chen and R. C. Haddon, *Appl. Phys. Lett.*, 1999, **75**, 1329–1331.
57 T. V. Sreekumar, T. Liu, B. G. Min, H. Guo, S. Kumar, R. H. Hauge and R. E. Smalley, *Adv. Mater.*, 2004, **16**, 58–61.
58 H. Zhang, Z. G. Wang, Z. N. Zhang, J. Wu, J. Zhang and J. S. He, *Adv. Mater.*, 2007, **19**, 698–704.
59 K. Liu, Y. Sun, X. Lin, R. Zhou, J. Wang, S. Fan and K. Jiang, *ACS Nano*, 2010, **4**, 5827–5834.
60 S. Garreau, G. Louarn, J. P. Buisson, G. Froyer and S. Lefrant, *Macromolecules*, 1999, **32**, 6807–6812.
61 D. Antiohos, G. Folkes, P. Sherrell, S. Ashraf, G. G. Wallace, P. Aitchison, A. T. Harris, J. Chen and A. I. Minett, *J. Mater. Chem.*, 2011, **21**, 15987–15994.
62 E. Frackowiak, V. Khomenko, K. Jurewicz, K. Lota and F. Béguin, *J. Power Sources*, 2006, **153**, 413–418.
63 G. A. Snook, P. Kao and A. S. Best, *J. Power Sources*, 2011, **196**, 1–12.
64 S. H. Aboutalebi, A. T. Chidembo, M. Salari, K. Konstantinov, D. Wexler, H. K. Liu and S. X. Dou, *Energy Environ. Sci.*, 2011, **4**, 1855–1865.
65 C. Y. Wang, V. Mottaghitalab, C. O. Too, G. M. Spinks and G. G. Wallace, *J. Power Sources*, 2007, **163**, 1105–1109.

